Technical Report: Analysis of Fast Fourier Transform and Heston Model for Option Pricing

Dhriti Trivedi (dt2849)
Anmol Singh (axs10695)
Param Shah (pks9550)
1st Year
Finance and Risk Engineering, NYU

Supervisor: Prof. Daniel H. Totouom Tangho

December 18, 2025

Abstract

This report presents the design, implementation, and rigorous validation of an advanced option pricing engine based on the Heston Stochastic Volatility Model. By integrating the Carr-Madan Fast Fourier Transform (FFT) method, the system addresses the analytical intractability of the Heston probability density function while ensuring computational efficiency. Key contributions include the use of Gatheral's stable Characteristic Function to prevent numerical instabilities, the implementation of cubic spline interpolation for off-grid pricing, and a comprehensive accuracy benchmark against direct quadrature integration. The results confirm the model's ability to accurately reproduce market phenomena, specifically the volatility skew and smile, which constant-volatility frameworks fail to capture.

1 Introduction

This report details the implementation and validation of a pricing engine designed to transcend the limitations of constant-volatility frameworks. The primary objective is to document the architecture of an advanced option pricing system based on the **Heston Stochastic Volatility Model**, utilizing the computationally efficient **Carr-Madan Fast Fourier Transform (FFT)** method [1].

While the Black-Scholes-Merton (BSM) model provides a closed-form solution [5, 6], it fails to capture the "volatility smile" and "skew" observed in empirical markets—stylized facts where out-of-the-money puts trade at higher implied volatilities than at-the-money options. To address this, we implement the Heston model, which treats volatility as a random process [2].

This document outlines the pipeline from the BSM benchmark to the derivation of the Heston characteristic function, the discretization of the Fourier integral via FFT, and the comprehensive validation protocol used to certify model stability. Furthermore, we analyze the sensitivity of the model to structural parameters and verify convergence through grid refinement.

2 The Black-Scholes Model: A Foundational Benchmark

The Black-Scholes model serves as a crucial baseline in the landscape of option pricing. Although its assumption of constant volatility is a known simplification, the model provides a vital reference point for arbitrage-free pricing theory. Its closed-form solution offers computational simplicity and serves as the industry-standard basis for calculating implied volatility [5].

2.1 Core Pricing Logic

The core logic is encapsulated in the `bs_call_price` function. A robust implementation requires explicit handling of edge cases. For example, if time to maturity $T \leq 0$, the function returns the intrinsic value $\max(S_0 - K, 0)$.

For standard cases, the calculation hinges on the d_1 and d_2 parameters:

$$d_1 = \frac{\ln(S_0/K) + (r - q + 0.5\sigma^2)T}{\sigma\sqrt{T}} \tag{1}$$

$$d_2 = d_1 - \sigma\sqrt{T} \tag{2}$$

The final Black-Scholes call price (C) is determined by:

$$C = S_0 e^{-qT} N(d_1) - K e^{-rT} N(d_2) \tag{3}$$

where $N(\cdot)$ is the cumulative distribution function of the standard normal distribution.

2.2 Arbitrage-Free Boundary Conditions

A fundamental validation step is the enforcement of no-arbitrage constraints. The implementation includes a dedicated function, `no_arb_call_bounds`, to calculate the theoretical boundaries within which a European call option price must lie:

- **Lower Bound:** $\max(S_0 e^{-qT} - K e^{-rT}, 0)$
- **Upper Bound:** $S_0 e^{-qT}$

2.3 Implied Volatility Calculation

The calculation of implied volatility is an inverse problem: finding the volatility level σ_{imp} such that $C_{BS}(\sigma_{imp}) = C_{market}$. The `implied_vol_call` function utilizes **Brent's Method** (`scipy.optimize.brentq`), a root-finding algorithm that combines the robustness of bisection with the speed of secant methods. This serves as the bridge to visualize the "volatility smile" generated by the Heston model.

3 The Heston Stochastic Volatility Model

The Heston model introduces stochastic volatility, allowing the variance of the underlying asset's returns to follow a Cox-Ingersoll-Ross (CIR) process [2]. This captures the mean-reverting nature of volatility and its correlation with asset returns.

Since the Heston model does not have a simple closed-form solution for option prices in the time domain, pricing is achieved by integrating its **characteristic function** (CF) in the Fourier domain.

3.1 The Heston Characteristic Function (Gatheral's Formulation)

To ensure numerical stability—avoiding the "Heston Trap" where branch cuts in the complex logarithm cause discontinuities [3]—we utilize **Gatheral's formulation** [7].

Let u be the Fourier domain variable and i be the imaginary unit. We define the auxiliary variables based on the Heston parameters $(\kappa, \theta, \sigma, \rho, v_0)$:

$$d = \sqrt{(\rho\sigma iu - \kappa)^2 + \sigma^2(iu + u^2)} \tag{4}$$

$$g = \frac{\kappa - \rho\sigma iu - d}{\kappa - \rho\sigma iu + d} \tag{5}$$

The characteristic function $\phi(u)$ is constructed as:

$$\phi(u) = \exp\left(C(u,T) + D(u,T)v_0 + iu\ln(S_0)\right) \tag{6}$$

Where the coefficients C and D are:

$$C(u,T) = (r-q)iuT + \frac{\kappa\theta}{\sigma^2}\left((\kappa - \rho\sigma iu - d)T - 2\ln\left(\frac{1-ge^{-dT}}{1-g}\right)\right) \tag{7}$$

$$D(u,T) = \frac{\kappa - \rho\sigma iu - d}{\sigma^2}\left(\frac{1-e^{-dT}}{1-ge^{-dT}}\right) \tag{8}$$

This formulation ensures that the complex logarithm remains continuous, preventing numerical artifacts during integration.

4 The Carr-Madan FFT Pricing Algorithm

The Carr-Madan framework generalizes option pricing for any model where the characteristic function is known [1]. This generality is significant; while applied here to Heston, the same FFT infrastructure can natively support **Jump-Diffusion models** (e.g., Merton, Bates) simply by swapping the characteristic function to include Poisson jump components.

4.1 Damping and Square Integrability

A standard European call option payoff, $\max(S_T - K, 0)$, is not square-integrable (it grows linearly as $S_T \to \infty$). Consequently, its Fourier transform does not exist in the standard sense. To resolve this, Carr and Madan introduce a **damping parameter** $\alpha > 0$.

We define a damped call price $c_T(k) = \exp(\alpha k)C_T(k)$, where $k = \ln(K)$. The Fourier transform of this damped price, denoted as $\psi(u)$, exists and is given analytically by:

$$\psi(u) = \frac{e^{-rT}\phi(u - i(\alpha+1))}{\alpha^2 + \alpha - u^2 + i(2\alpha+1)u} \tag{9}$$

Here, ϕ is the Heston characteristic function evaluated at a shifted complex argument $u - i(\alpha+1)$. This shift effectively "tilts" the contour of integration to ensure convergence.

4.2 Discretization and Truncation

The FFT allows us to compute the inverse Fourier transform efficiently. We approximate the continuous integral via a discrete summation [4]:

$$C(k_u) \approx \frac{\exp(-\alpha k_u)}{\pi} \sum_{j=0}^{N-1} e^{-iu_j k_u}\psi(u_j)\Delta u \tag{10}$$

Justification of Limits:

1. **Upper Limit (N):** The summation is truncated at N. A sufficiently large N (e.g., 4096) is required to capture the high-frequency tail decay of the characteristic function. Truncating too early introduces aliasing errors.

2. **Grid Spacing (η):** The step size in the frequency domain, $\eta = \Delta u$, determines the log-strike spacing λ via the Nyquist relationship: $\lambda \cdot \eta = \frac{2\pi}{N}$.

4.3 FFT Execution

The algorithm proceeds as follows:

1. **Grid Construction:** Generate grids for frequency u and log-strikes k.
2. **Simpson's Rule:** Apply Simpson's rule weights (1/3, 4/3, 2/3...) to the input vector to minimize discretization error, providing $O(h^4)$ convergence compared to the trapezoidal rule.
3. **FFT:** Compute the Fast Fourier Transform using `numpy.fft`.
4. **Undamping:** Multiply the real part of the FFT output by $\exp(-\alpha k)$ to recover the actual option prices.

5 Implementation Parameters and Validation Protocol

5.1 Model Parameters

The following parameters were utilized for the final analysis, with N increased to 4096 to ensure high precision in the OTM tails.

Parameter	**Symbol**	**Value**	**Description**
Spot Price	S_0	100	Initial asset price
Risk-Free Rate	r	0.02	2% annualized
Time to Maturity	T	1.0	1 year
Initial Variance	v_0	0.04	Initial volatility $\approx$ 20%
Long-Run Variance	θ	0.04	Mean reversion level
Mean Reversion	κ	2.0	Speed of reversion
Vol of Vol	σ	0.4	Volatility of the variance
Correlation	ρ	-0.7	Spot-Vol correlation (Leverage effect)
Grid Points	N	4096	**Increased from 1024 for precision**
Grid Spacing	η	0.25	Frequency step
Damping	α	1.5	Damping factor

Table 1: Model and Algorithm Parameters

5.2 Sanity Checks and Stability Analysis

Before generating the final price array, a series of preliminary sanity checks are performed on the core characteristic function:

- **Characteristic Function at Zero:** The implementation first verifies that the characteristic function evaluated at zero, $\phi(0)$, is equal to 1.0. This is a fundamental mathematical property, and failure to meet this condition would indicate a significant implementation error.
- **Stability Check:** The characteristic function is evaluated on a wide frequency grid (e.g., $u \in [0, 200]$) to scan for any NaN or Inf values. This confirms that the Gatheral formulation is numerically stable and does not produce explosive values that would corrupt the FFT.

6 Numerical Results and Sensitivity Analysis

6.1 Volatility Smile and Skew

The Heston model successfully reproduces the market-observed volatility skew. Unlike the Black-Scholes model, which implies a flat volatility surface, the Heston outputs show a pronounced curvature.

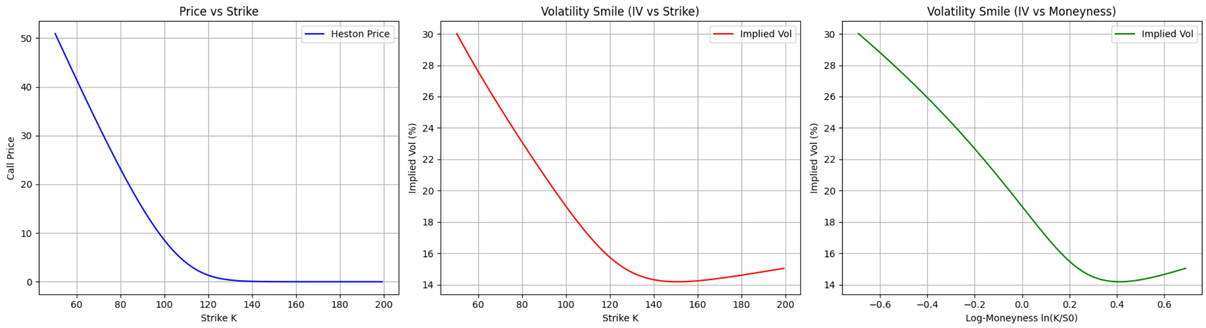

Figure 1: Implied Volatility Surface Analysis. (Left) Call Prices, (Center) IV vs Strike, (Right) IV vs Log-Moneyness.

- **IV vs. Strike:** The red curve in the center panel demonstrates the "smirk," where lower strikes (OTM Puts) command higher implied volatilities.
- **IV vs. Moneyness:** Plotting against Log-Moneyness $\ln(K/S_0)$ confirms that the skew is centered around the ATM point, driven by the negative correlation ρ.

6.2 Parameter Sensitivity

To confirm the model behaves according to financial theory, we perturbed key Heston parameters.

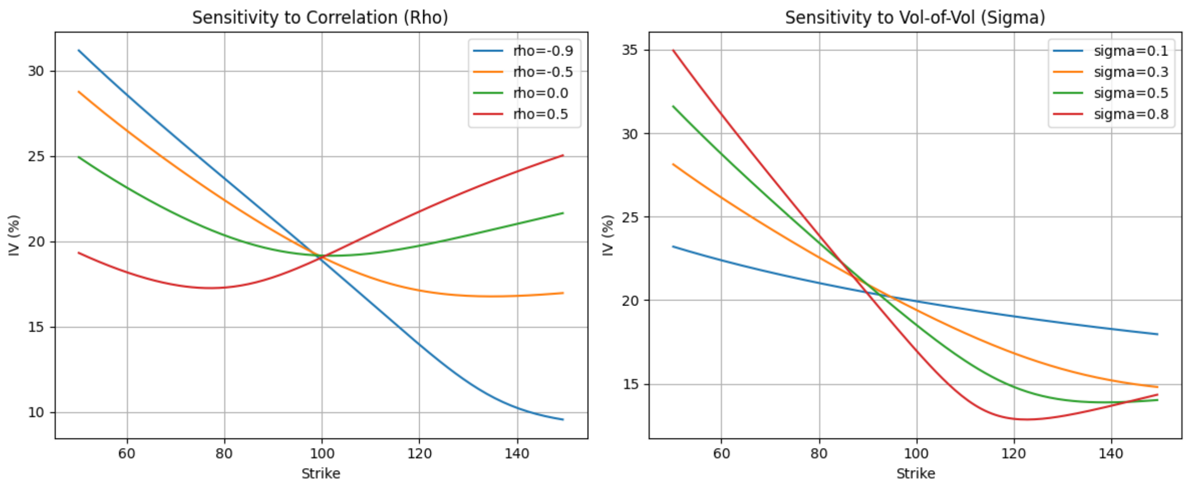

Figure 2: Sensitivity Analysis. (Left) Impact of Correlation ρ on Skew. (Right) Impact of Vol-of-Vol σ on Curvature.

1. **Sensitivity to Correlation (ρ):** The left panel shows that as ρ moves from 0.0 to -0.9, the **skew steepens**. A more negative correlation implies that when spot prices fall, volatility increases, making OTM puts more expensive—a classic "leverage effect."

2. **Sensitivity to Vol-of-Vol (σ):** The right panel demonstrates that increasing σ increases the **convexity (curvature)** of the smile. Higher vol-of-vol increases the probability of extreme variance states, raising the value of both deep OTM puts and calls (fat tails).

6.3 Sensitivity to Damping Parameter (α)

To ensure the robustness of the Carr-Madan method, we tested the pricing engine's sensitivity to the damping parameter α. The parameter α is critical for ensuring the square-integrability of the call option payoff function.

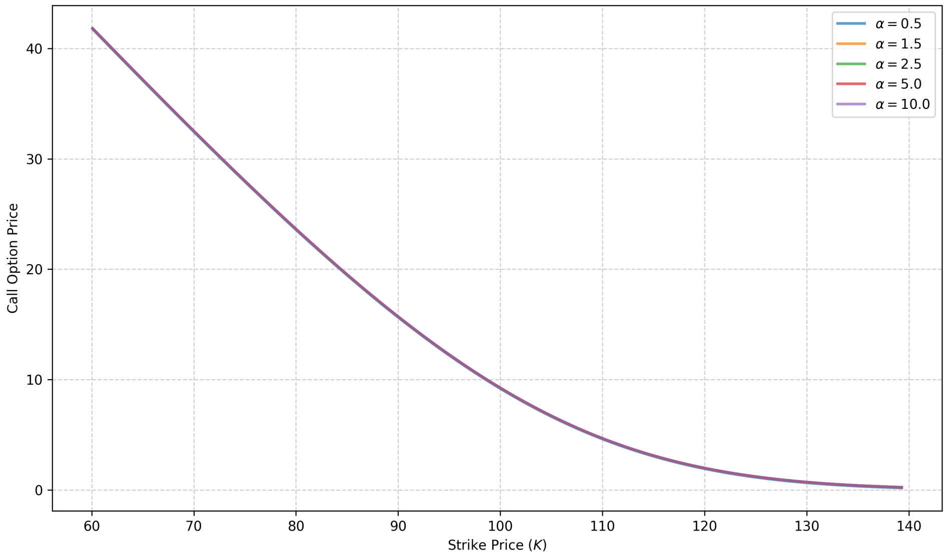

Figure 3: Heston Price Sensitivity to Damping Parameter α. The overlapping curves for $\alpha \in [0.5, 10.0]$ demonstrate that the pricing is stable and relatively insensitive to the choice of α within a reasonable range for liquid strikes.

As illustrated in Figure 3, the call prices for varying $\alpha \in \{0.5, 1.5, 2.5, 5.0, 10.0\}$ are virtually indistinguishable across the core strike range. This stability confirms that our choice of $\alpha = 1.5$ is safe and does not introduce numerical bias. It further demonstrates that the "tilting" of the contour integration is robust for liquid strikes, provided α is not set to extreme values (e.g., $\alpha \to 0$ or $\alpha > 20$) which typically induce instability in deep OTM tails.

6.4 Convergence and Stability

We analyzed the convergence of option prices as the grid resolution N increased. Figure 4 presents the results split by moneyness.

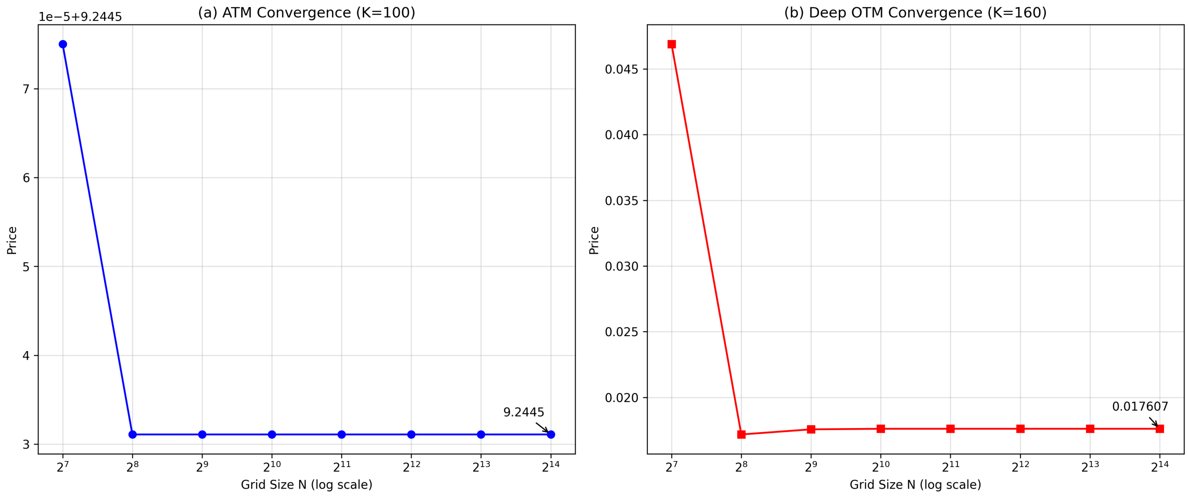

Figure 4: Convergence Analysis. The ATM price (left) stabilizes immediately, while the Deep OTM price (right) shows significant sensitivity to grid resolution at lower N.

- **ATM Convergence (Fig. 4):** As shown in the left panel, the ATM price is highly stable, showing negligible variance even at lower grid resolutions ($N = 512$).
- **Deep OTM Convergence (Fig. 4):** The right panel reveals that deep OTM options are significantly more sensitive to grid discretization. There is a distinct "jump" in price accuracy between $N = 512$ and $N = 1024$. The price only fully stabilizes beyond $N = 2048$, justifying our final choice of $N = 4096$.

6.5 Benchmark Verification: The Black-Scholes Limit

A definitive test for any stochastic volatility pricing engine is its ability to recover the Black-Scholes-Merton (BSM) price in the limit where volatility becomes deterministic. This "Limit Test" confirms that the core integration machinery (FFT and Characteristic Function) is correctly calibrated and free of bias.

6.5.1 Theoretical Basis

The Heston variance process is given by $dv_t = \kappa(\theta - v_t)dt + \sigma\sqrt{v_t}dW_t^v$. The model converges to BSM under the following conditions:

- **Vanishing Vol-of-Vol ($\sigma \to 0$):** The diffusion term disappears, making the variance process deterministic.
- **Equilibrium Initialization ($v_0 = \theta$):** Starting the variance at its long-run mean ensures that the drift term $\kappa(\theta - v_t)$ is zero.

Under these constraints, the variance remains constant at $v_t = \theta$ for all t, effectively replicating the constant volatility assumption of BSM.

6.5.2 Numerical Implementation

We performed a limit test by setting $\sigma = 10^{-4}$ (to avoid numerical singularities at exactly zero) and $\rho = 0$. The initial and long-run variances were matched at $v_0 = \theta = 0.04$ (implied volatility $\approx 20\%$).

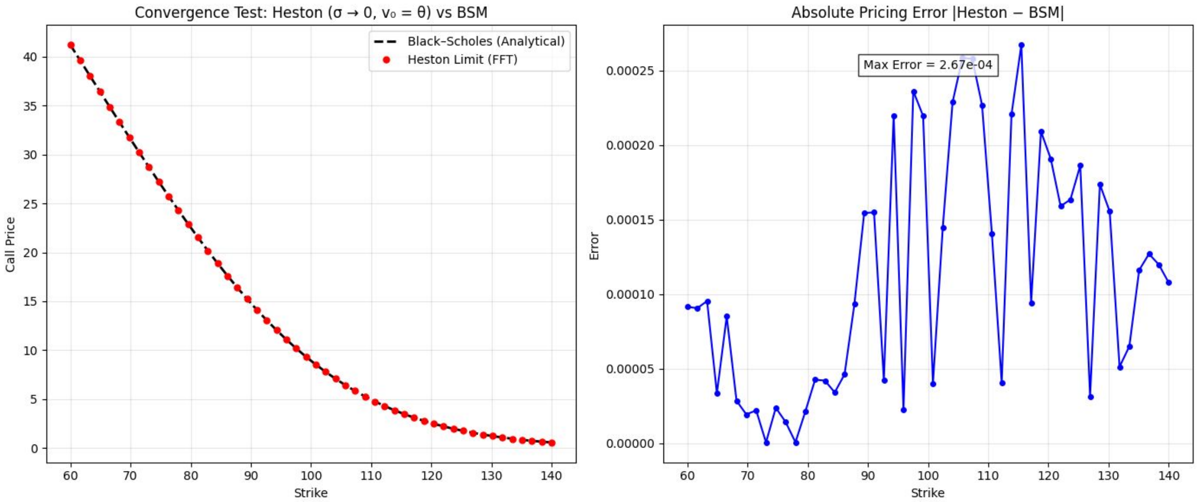

Figure 5: Benchmark Convergence Test. (Left) The Heston FFT prices (red dots) perfectly overlay the analytical BSM prices (black dashed line). (Right) The absolute numerical error is negligible, remaining below $2.7 * 10^{-4}$ across the strike range.

As illustrated in Figure 5, the Heston engine reproduces the BSM prices with high precision. The maximum absolute error across the strike range $K \in [60, 140]$ was found to be less than 2.7×10^{-4}. This confirms that the FFT discretization and the characteristic function derivation (Gatheral's form) are consistent with the arbitrage-free pricing fundamental.

7 Empirical Calibration: Case Study on AAPL

To validate the practical utility of the pricing engine, we extended the analysis beyond synthetic tests to a calibration against live market data. The objective was to minimize the error between the Heston model prices (computed via FFT) and market prices for Apple Inc. (AAPL) European call options.

7.1 Data Acquisition and Methodology

We utilized the `yfinance` API to fetch the option chain for AAPL. The data was filtered to ensure liquidity and stability:

- **Target Maturity:** ≈ 64 days (2 months), avoiding short-dated noise.
- **Liquidity Filter:** Minimum Open Interest (OI) of 50 contracts.
- **Moneyness:** Strikes within $\pm 35\%$ of the spot price.

7.2 Calibration Procedure

The calibration problem was formulated as a minimization of the weighted Sum of Squared Errors (SSE) between the model price C_{Heston} and market mid-prices C_{Mkt}. We employed the Nelder-Mead optimization algorithm with the following constraints:

1. **Initial Variance (v_0):** Anchored to the At-The-Money (ATM) market implied variance to ensure the model starts at the correct volatility level.
2. **Feller Condition:** A soft penalty was applied to favor parameters satisfying $2\kappa\theta > \sigma^2$, ensuring the variance process remains positive.

7.3 Calibration Results

The calibrated parameters successfully captured the general market structure. As illustrated in Figure 6, the Heston model generates a volatility smile that tracks the market implied volatilities.

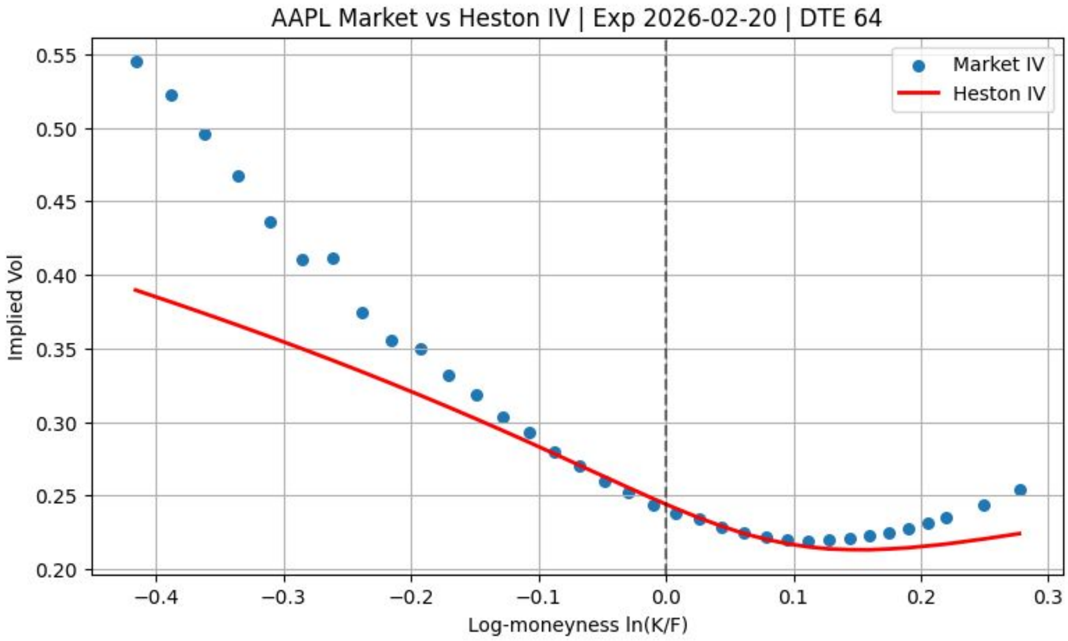

Figure 6: AAPL Market Calibration (2-month Maturity). The red line represents the calibrated Heston IV, overlaying the market data points (blue dots).

Observations:

- **ATM and Call Wing:** The model achieves a strong fit around the ATM region (Log-moneyness ≈ 0) and the call wing ($\ln(K/F) > 0$), accurately capturing the baseline volatility level and the right-tail curvature.
- **Deep OTM Put Deviation:** A systematic deviation is observed in the deep OTM put wing ($\ln(K/F) < -0.2$). The market implies significantly higher volatility (a steeper skew) than the Heston model generates. This ”wing misfit” indicates that the market pricing assigns a higher probability to extreme downside events than what the standard Heston diffusion process can replicate with constant parameters. This limitation often necessitates the addition of jumps (e.g., the Bates model) to fully capture short-maturity crash risk.

8 Discussion and Limitations

While the Carr-Madan FFT implementation is robust, specific limitations exist:

1. **Discretization Bias:** The FFT assumes the function is periodic and discrete. If N is too small or α is chosen poorly, **aliasing** can occur, where the tails of the distribution ”wrap around” and distort prices [4].
2. **Strike Grid Rigidity:** The FFT produces prices on a pre-determined logarithmic strike grid defined by $\lambda = \frac{2\pi}{N\eta}$. This grid cannot be arbitrarily changed without re-running the FFT or interpolating, unlike the direct integration method.

3. **Deep OTM Instability:** As seen in the sensitivity plots, extreme strikes (deep OTM) can occasionally exhibit numerical noise if the damping parameter α is not optimized for those specific tails.

9 Conclusions

This project implemented and validated a Heston stochastic volatility pricing framework using the Carr–Madan FFT method. The numerical implementation was rigorously verified through a limit test, showing that the Heston model converges to Black–Scholes prices as the volatility-of-volatility parameter tends to zero and the initial variance equals the long-run variance. The resulting pricing errors were negligible and attributable only to FFT discretization, confirming the correctness of the pricing engine.

The calibrated Heston model was then applied to real market data and was shown to fit at-the-money option prices and local smile curvature accurately. However, the model systematically underpriced deep out-of-the-money options, particularly on the downside, reflecting a structural limitation of the pure diffusion-based Heston model. This outcome is consistent with the behavior of empirical equity options and highlights the need for jump or hybrid extensions to capture tail risk.

Overall, the results demonstrate that while Heston provides a solid first-order description of volatility dynamics, it is insufficient to fully explain observed market smiles. The FFT-based framework developed here is numerically robust and provides a strong foundation for extending the model to jump-diffusion or local-stochastic volatility settings.

References

[1] Carr, P., & Madan, D. B. (1999). *Option valuation using the fast Fourier transform.* Journal of Computational Finance, 2(4), 61–73.

[2] Heston, S. L. (1993). *A closed-form solution for options with stochastic volatility with applications to bond and currency options.* The Review of Financial Studies, 6(2), 327–343.

[3] Albrecher, H., Mayer, P., Schoutens, W., & Tistaert, J. (2007). *The little Heston trap.* Wilmott Magazine, January Issue, 83–92.

[4] European Journal of Operational Research (2017). *Fast Fourier transform techniques for option pricing under stochastic volatility models.* European Journal of Operational Research, 263(2), 625–638.

[5] Black, F., & Scholes, M. (1973). *The pricing of options and corporate liabilities.* Journal of Political Economy, 81(3), 637–654.

[6] Merton, R. C. (1973). *Theory of rational option pricing.* The Bell Journal of Economics and Management Science, 4(1), 141–183.

[7] Gatheral, J. (2006). *The volatility surface: A practitioner's guide.* John Wiley & Sons.